Coordination Geometries and Vibrational Properties of Cytochromes *a* and a_3 in Cytochrome Oxidase from Soret Excitation Raman Spectroscopy†

Gerald T. Babcock,* Patricia M. Callahan, Mark R. Ondrias,‡ and Irving Salmeen‡

ABSTRACT: Raman spectra have been recorded for oxidized, reduced, and inhibitor complexed cytochrome oxidase species. By judicious choice of laser excitation frequency in relation to the Soret optical absorption properties of cytochromes *a* and a_3, we have been able to enhance selectively and identify characteristic vibrations of the two iron chromophores. On the basis of a comparison of these assignments to Raman spectra of heme *a* model compounds, we conclude that cytochrome a_3 is six-coordinate and high-spin in the oxidized enzyme but five-coordinate and high-spin in the reduced protein; cytochrome *a* is six-coordinate and low-spin in both redox states of the enzyme. Cytochrome a_3 appears to be in a hydrophobic environment in its common valence states. In oxygenated cytochrome oxidase, formed by air oxidation of the reduced enzyme, cytochrome a_3^{3+} shows vibrational frequencies similar to those exhibited by low-spin heme *a* species. This suggests that a significant contraction in a_3 porphyrin core size accompanies the formation of this species. These coordination geometries are discussed with respect to the structure of the cytochrome a_3 site. We have used five laser lines which are in resonance with the Soret absorption band to construct a crude Raman excitation profile for reduced cytochrome oxidase. The experimental data are qualitatively in accord with the theoretical predictions of a Franck–Condon scattering mechanism; observed deviations from simple Franck–Condon behavior may be due to nonadiabatic effects, although this possibility has not been explored quantitatively. We have also studied cytochrome oxidase photoreduction and find that it can be explained by electron donation to the oxidase by a photogenerated reductant external to the protein metal centers. We find no evidence to suggest an unusual valence state for the iron of cytochrome a_3 in the resting enzyme.

In current models for the respiratory protein cytochrome oxidase, the metal centers of the enzyme are considered to function in pairs: low-spin cytochrome *a* and one of the coppers, Cu_a, are associated with cytochrome *c* oxidation while high-spin cytochrome a_3 and the second copper, Cu_{a_3}, are involved with dioxygen reduction [see Malmström (1979) for a review and Seiter & Angelos (1980) for an alternate view]. In the resting enzyme, a bridging, but unidentified, ligand is thought to mediate a strong exchange coupling between the ferric iron of cytochrome a_3 and Cu_{a_3} (Palmer et al., 1976; Blumberg & Peisach, 1979; Reed & Landrum, 1979; Stevens et al., 1979; Brudvig et al., 1980; Petty et al., 1980). The structure around the iron of cytochrome *a* is less controversial and most likely involves histidine ligands in the fifth and sixth positions of the heme *a* chromophore (Babcock et al., 1979; Blumberg & Peisach, 1979). In addition to its role in catalyzing dioxygen reduction, two other interesting and unusual aspects of the protein have emerged recently. The first is that the protein functions as a proton pump during respiration and contributes to the buildup of the membrane free energy gradient both by consuming protons during oxygen reduction and by translocating protons from the inner to the outer aqueous space (Wikström & Krab, 1979). The second is that the redox properties of cytochromes *a* and a_3 are interdependent, and events at the iron of one of the centers can alter the redox potential of the second (Babcock et al., 1978). The molecular bases for these two phenomena are unknown.

Raman spectroscopy offers the potential to resolve several of the outstanding questions regarding this enzyme. The technique provides information on both the immediate coordination sphere of the heme-bound iron (Spaulding et al., 1975; Spiro et al., 1979; Callahan & Babcock, 1981) and the conformation of porphyrin ring peripheral substituents (Salmeen et al., 1973, 1978). Given the unusual formyl substituent of heme *a*, this latter insight is expected to be extremely useful (Babcock & Salmeen, 1979). The application of Raman spectroscopy to the enzyme, however, is complicated by facile photoreduction of the metal centers in the laser beam (Adar & Yonetani, 1978; Adar & Erecińska, 1979) and by ambiguities in the optical properties of the two heme chromophores. The photoreduction difficulty has been avoided recently by using frozen samples and laser excitation in the visible region (Bocian et al., 1979) or by using flowing oxidase samples (Babcock & Salmeen, 1979). Using the flow technique and several Soret region laser lines to obtain oxidase Raman spectra, we have been able to clarify the optical properties of cytochromes *a* and a_3 (Babcock & Salmeen, 1979; Ondrias & Babcock, 1980). Recent oxidase Raman studies carried out by Woodruff et al., (1981) have confirmed these observations. The absorption properties of cytochromes *a* and a_3 determined by Raman spectroscopy are in close agreement with those originally postulated by Vanneste (1966) but which had been clouded somewhat during the past decade by the uncertain manifestations of heme–heme interaction (Malmström, 1979).

The majority of the oxidase Raman work we have done has used Soret excitation. The scattered intensity under these conditions is controlled by Franck–Condon overlap factors and is distinct from the Herzberg–Teller nature of heme Raman spectra obtained with excitation in resonance with the α and β bands (Felton & Yu, 1978; Rousseau et al., 1979; Clark & Stewart, 1979). In the preceding paper we showed that Soret excitation Raman spectroscopy can be used to extract heme structural information provided suitable model compound data are available (Callahan & Babcock, 1981). In the present paper, we assign vibrational bands for cytochromes *a* and a_3

† From the Department of Chemistry, Michigan State University, East Lansing, Michigan 48824 (G.T.B., P.M.C., and M.R.O.), and the Research Staff, Chemical Sciences, Ford Motor Company, Dearborn, Michigan 48121 (I.S.). *Received July 16, 1980.* The portion of this investigation which was carried out at Michigan State University was supported by National Institutes of Health Grant No. GM25480.

‡ General Electric Summer Fellow. Present address: Bell Telephone Laboratories, Murray Hill, NJ 07974.

0006-2960/81/0420-0959$01.00/0

and use these in conjunction with heme *a* model compound data to determine spin and coordination states for the two oxidase iron chromophores. We have also explored the Soret excitation frequency dependence of the reduced oxidase Raman spectrum and show that this can be interpreted qualitatively by assuming that the polarizability is dominated by a single electronic state and its Franck–Condon overlap with the ground state. Finally, we have studied in some detail the mechanism of cytochrome oxidase photoreduction in order to clarify the nature of this process and to test a recent proposal concerning the valence of the metal centers in the resting enzyme (Seiter & Angelos, 1980). A preliminary account of some of the research described here has been given elsewhere (Babcock et al., 1980).

Materials and Methods

Beef heart cytochrome oxidase was isolated and its inhibitor complexes were prepared as described previously (Babcock et al., 1976; Babcock & Salmeen, 1979). The standard buffer–detergent system consisted of 0.05 M Hepes[1] and 0.5% Brij 35, pH 7.4 and was used in all experiments except where noted. Rat liver cytochrome oxidase was generously supplied by Professor S. Ferguson-Miller. The buffer for the rat liver enzyme consisted of 0.05 M Tris–HCl, 0.33 M sucrose, 0.001 M histidine, 0.2 M potassium phosphate, and 0.015 M lauryl maltoside, pH 8.0.

Raman spectra were obtained with the spectrometer described in the preceding paper (Callahan & Babcock, 1981) and either krypton ion (Spectra Physics 164-11 equipped with high-field magnet and blue optics), argon ion (Spectra Physics 165), or helium–cadmium (RCA LD2186) lasers. The power incident on the sample was measured with a Coherent Radiation power meter (Model No. 210) and was typically 10–20 mW except where noted. For static samples, the temperature was maintained at 4 °C by cold flowing nitrogen gas; for flowing oxidase samples the temperature was maintained at 11 °C. Sample concentrations were generally varied between 10 and 50 μM so as to provide an absorbance of between 1 and 2 at the excitation wavelength. However, for the protein samples used to obtain the excitation profile data of Figure 2, the oxidase concentration was maintained at 14 μM, and 0.12 M $(NH_4)_2SO_4$ was added as an internal standard. Control experiments showed that the presence of the ammonium sulfate did not alter the Raman scattering properties of the enzyme. Reabsorption effects were estimated to lead to maximum errors in the determination of scattered intensity of <8% but were not corrected for. The detector response of the RCA C31034 tube used is essentially frequency independent over the spectral range of interest. Optical spectra were recorded before and after the Raman experiment in order to monitor sample integrity.

Results

Soret Raman Scattering Frequency Dependence. Studies concerned with the frequency dependence of Raman scattering in the α,β region of heme protein electronic spectra have been carried out, for example, on cytochrome *c* (Friedman et al., 1977), and have been interpreted to first order in terms of a Herzberg–Teller scattering mechanism, and more quantitatively by incorporating both nonadiabatic and Jahn–Teller effects (Shelnutt, 1980). No systematic investigations of this type have been carried out for Soret excitation, with the exception of a study carried out by Champion & Albrecht (1979) on the oxidation state marker band of cytochrome *c*. Because the Soret absorption spectrum of cytochrome oxidase is considerably red shifted compared to other hemes and heme proteins, fixed-frequency ion laser lines can be used to construct a crude excitation profile in order to explore in more detail the frequency dependence of Soret scattering.

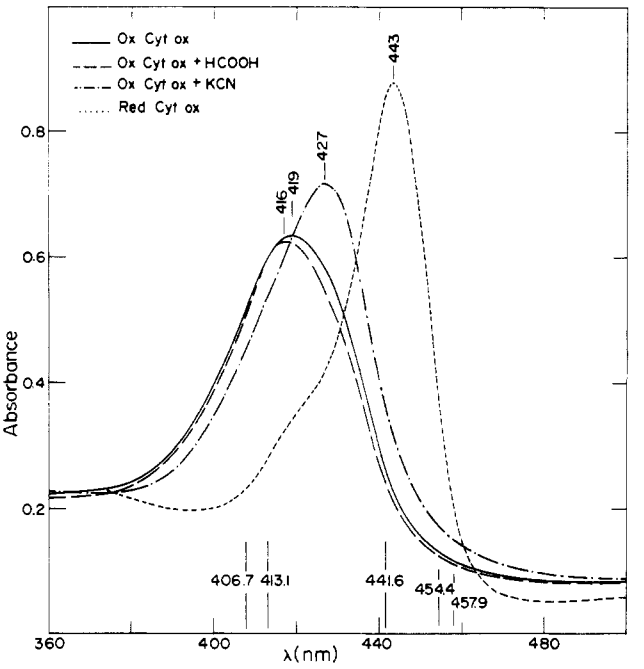

FIGURE 1: Optical absorption spectra of several of the cytochrome oxidase species used in the Raman experiments reported here. The wavelengths of the laser lines available are also shown in the figure. The cytochrome oxidase concentration was ~4 μM (in enzyme) for all four compounds.

Figure 1 shows the optical spectra of several of the oxidase derivatives used in the present study and the relationship of the five available laser lines to these spectra. In reduced cytochrome oxidase, both a^{2+} and a_3^{2+} have maxima at 443 nm (Vanneste, 1966). Two of the laser lines are thus on the long-wavelength side of the absorption peak (by 571 and 735 cm^{-1}), and the remaining three are on the short-wavelength side of the peak (by 71, 1634, and 2015 cm^{-1}). Figure 2 shows Raman spectra of the reduced oxidase obtained with the three highest frequency lines as well as the Raman spectrum of reduced rat liver cytochrome oxidase with 441.6-nm excitation. The spectra obtained with the 457.9- and 454.5-nm lines were similar to those recorded by Nafie et al. (1973). We present a brief discussion of these data here since it will be useful in considering other data presented below.

The intensity of Raman scattering is determined by the polarizability tensor which has a form near resonance given by

$$\alpha_{\rho\sigma} = \sum_{i,\nu} \frac{\langle gn|R_\sigma|i\nu\rangle\langle i\nu|R_\rho|gn'\rangle}{E^{i\nu} - E^{gn} - h\nu - i\Gamma_{i\nu}} \qquad (1)$$

where $E^{i\nu}$ and $\Gamma_{i\nu}$ are the energy and homogeneous line width of the excited vibronic state $|i\nu\rangle$, respectively, E^{gn} is the energy of the ground vibronic state $|gn\rangle$, R_ρ and R_σ are electric dipole moment operators with ρ and $\sigma = x, y$, and z and the summation excludes the ground vibronic states $|gn\rangle$ and $|gn'\rangle$, and the incident photon energy is $h\nu$ (Felton & Yu, 1978). Albrecht & Hutley (1971) have shown that this can be expanded

[1] Abbreviations used: Me_2SO, dimethyl sulfoxide; EPR, electron paramagnetic resonance; Hepes, *N*-(2-hydroxyethyl)piperazine-*N'*-2-ethanesulfonic acid; MCD, magnetic circular dichroism; Tris, tris(hydroxymethyl)aminomethane; NMeIm, *N*-methylimidazole.

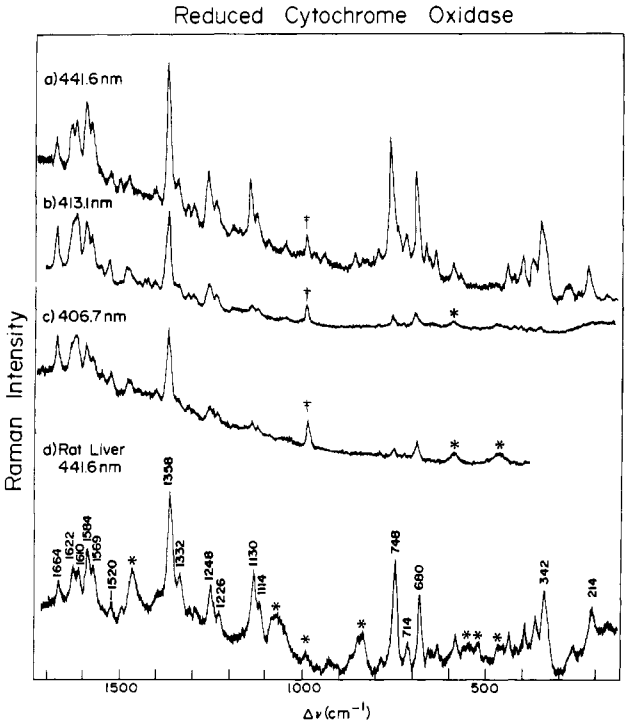

FIGURE 2: Raman spectra of reduced beef heart cytochrome oxidase (a, b, and c) and of reduced rat liver cytochrome oxidase (d) recorded with the laser lines indicated. Instrumental conditions: resolution, 6 cm^{-1}; time constant, 1 s; scan rate, 50 cm^{-1}/min. Raman lines which originate from the buffer systems used are indicated by asterisks; the daggers indicate the Raman line of the sulfate internal standard.

if the Born–Oppenheimer approximation is used and that the resulting expression, excluding nonadiabatic effects, can be represented as the sum of two terms

$$\alpha_{\rho\sigma} = A_{\rho\sigma} + B_{\rho\sigma} \tag{2}$$

where the $A_{\rho\sigma}$ term represents Franck–Condon scattering and the $B_{\rho\sigma}$ term scattering by a Herzberg–Teller mechanism. Both Felton & Yu (1978) and Rousseau et al., (1979) have lucidly discussed the application of this formalism to heme protein Raman and have concluded that the B term describes, to first order, α- and β-band scattering and suggest that the A term should apply to Soret scattering. The Soret scattered intensity is then proportional to the square of the A term and is given by

$$I \simeq |A|^2 \simeq \left| \frac{\langle g0|i0\rangle}{E^{i0} - E^{g0} - h\nu - i\Gamma_{i0}} - \frac{\langle g1|i1\rangle}{E^{i1} - E^{g0} - h\nu - i\Gamma_{i1}} \right|^2 \tag{3}$$

where the ground-state and excited-state lowest vibronic levels are $|g0\rangle$ and $|i0\rangle$, respectively, with energies given by E^{g0} and E^{i0}; $|g1\rangle$ and $|i1\rangle$ represent ground and excited state vibronic levels one vibrational quantum above the lowest vibrational state.

This expression predicts two peaks in the Soret excitation profile for a given mode: one at the absorption peak (i.e., at the 0–0 fundamental) and a second at a frequency given by the sum of the 0–0 fundamental and the vibrational quantum.[2] Constructive interference is predicted in the frequency region between the two peaks, and destructive interference is predicted in the wings.

[2] In earlier work, we had used an approximate form of this equation obtained by equating $E^{i0} - E^{g0}$ and $E^{i1} - E^{g0}$ (Salmeen et al., 1978; Babcock & Salmeen, 1979; Ondrias & Babcock, 1980).

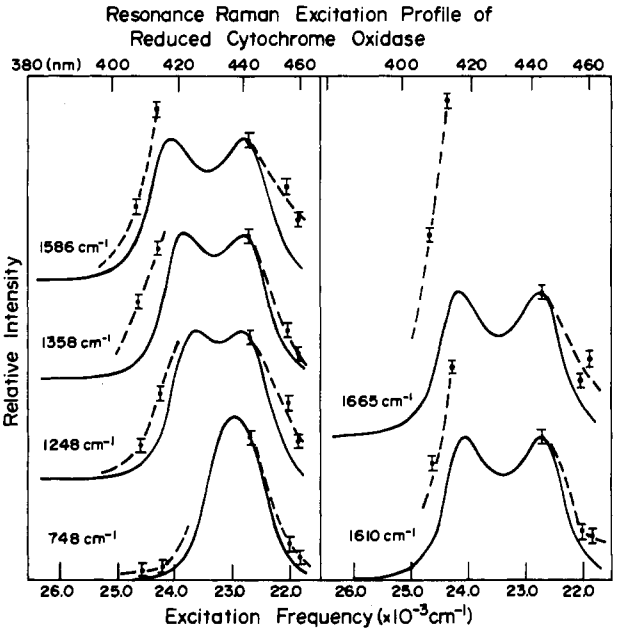

FIGURE 3: Raman excitation profiles for modes indicated have been calculated from eq 3 in the text and are shown by solid lines. the experimental data obtained with the five available laser lines are shown by the closed circles and estimated error bars. The experimental and theoretical points are arbitrarily normalized at 441.6 nm. The three low-frequency points and the two high-frequency points have been connected by dashed lines which have no theoretical basis.

In Figure 3 we have plotted the excitation profiles of six of the modes in Figure 2 according to a form of eq 3, where the Franck–Condon factors in the numerator are set equal and approximated by the extinction coefficient at the Soret maximum. The bandwidth chosen in eq 3 was 475 cm^{-1}, estimated from the optical data of Vanneste (1966). Two peaks are observed in the calculated excitation profiles unless the bandwidth is of the same magnitude as the vibrational quantum, in which case the peaks are not resolved. We have included in these theoretical plots data points obtained from the experimental data of Figure 2. There is rough agreement between the calculated and experimental points in that the decreased intensity observed for the low-frequency modes with 406.7- and 413.1-nm excitation is predicted. However, the experimental data also show deviations from eq 3: (a) the scattered intensity on the low-frequency side of the 0,0 peak and on the high-frequency side of the 0,1 peak is greater than that calculated from eq 3 which predicts destructive interference in these regions, (b) the amplitude of the 0,1 scattering is greater than that of the 0,0, and (c) the effects in (a) and (b) become more pronounced as the frequency of the vibration increases. These three phenomena have been observed in α,β-band excitation profiles of heme proteins and have been accounted for by including a nonadiabatic term to allow for the effects of Soret excited states (Shelnutt et al., 1976; Rousseau et al., 1979). However, it is unclear whether nonadiabatic effects will be pronounced with Soret excitation; experiments are in progress to examine this further.

Oxidized Enzyme and Its Photoreduction. Photoreduction of resting cytochrome oxidase by the incident laser light at the powers required for Raman spectroscopy is a major obstacle to the application of this technique to the oxidized enzyme. Moreover, uncertainty exists in the literature regarding both the mechanism (Seiter & Angelos, 1980) and manifestations (Woodruff et al., 1981) of cytochrome oxidase photoreduction. Figure 4 presents results obtained with the flowing sample technique we have developed to avoid the

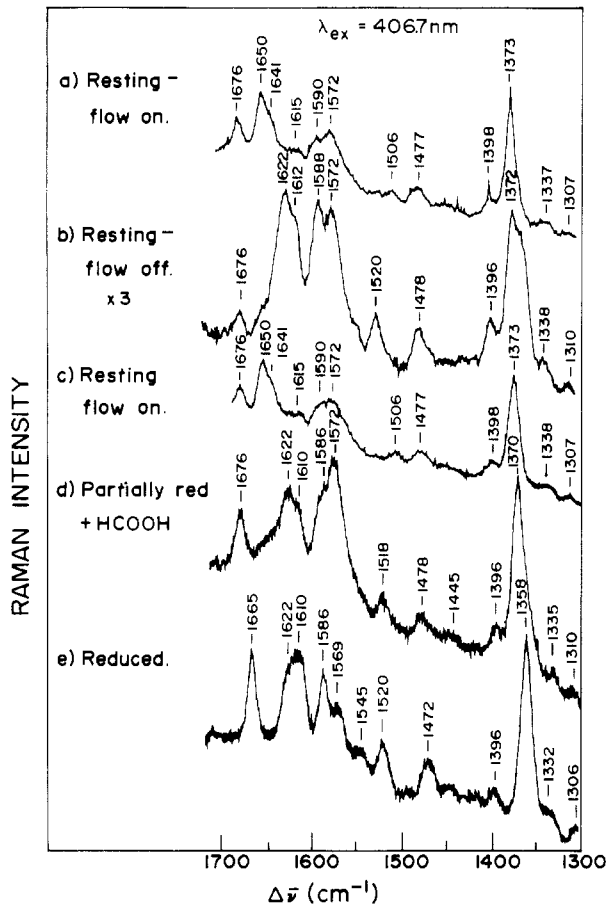

FIGURE 4: Resonance Raman spectra of several cytochrome oxidase species recorded with 406.7-nm excitation. Instrumental conditions: resolution, 6 cm^{-1}; time constant, 1 s; scan rate, 50 cm^{-1}/min. The instrument gain was constant in recording spectra a, c, d, and e; for spectrum b this was increased by a factor of 3.

photoreduction problem (Babcock & Salmeen, 1979). Under flow conditions (Figure 4a) and with 406.7-nm excitation the oxidation state marker band is observed at 1373 cm^{-1} with no shoulder to lower frequency, the oxidized cytochrome a_3 modes at 1572 and 1676 cm^{-1} are present (Ondrias & Babcock, 1980; see also below) and the cytochrome *a* modes at 1506 and 1590 cm^{-1} and near 1650 cm^{-1} are observed. (See Table I for a summary of the vibrational properties of cytochromes *a* and a_3.) When the flow is turned off and the spectrum of the static sample recorded (Figure 4b), a number of changes occur. In particular, new bands are apparent at 1622, 1612, and 1520 cm^{-1} and a shoulder appears on the low-frequency side of the 1372-cm^{-1} band. The cytochrome a_3^{3+} bands at 1676, 1572, and 1478 cm^{-1} are still present. The spectrum of the partially photoreduced enzyme in Figure 4b bears a strong resemblance to that of the enzyme in the presence of formate and a mild reductant (Figure 4d), a treatment which is known to generate the species $a^{2+}a_3^{3+}$·HCOOH (Nicholls, 1976). When the flow is restored, the sample again exhibits the spectrum of the oxidized enzyme (Figure 4c). We have noticed that there is a slight decrease in the intensity of the 1572-cm^{-1} band relative to the 1590-cm^{-1} band as the sample is illuminated in the flow system (compare parts a and c of Figure 4) which can be attributed to the formation of oxygenated cytochrome oxidase with time (see below). However, the kinetics of the conversion from oxygenated oxidase (λ_{max} = 427 mm) to the resting enzyme (λ_{max} = 420 nm) is faster in the Brij detergent we use than in other common solubilizing agents (Cholate, Tween), and hence the effects of oxygenation are minimized in the samples used in this study.[3]

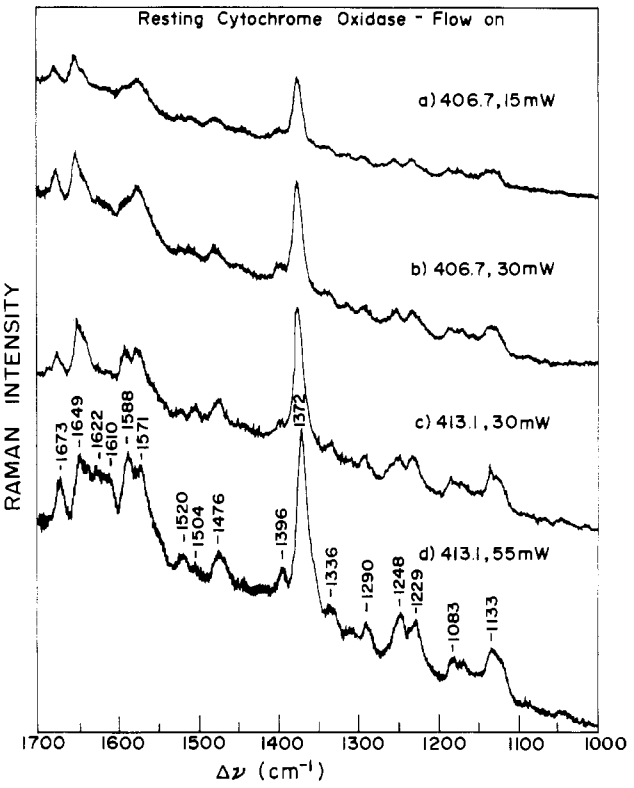

FIGURE 5: Incident laser power dependence of the resonance Raman spectrum of resting cytochrome oxidase. The excitation frequency and power incident on the sample are indicated. Instrumental conditions: resolution, 6 cm^{-1}; time constant, 1 s; scan rate, 50 cm^{-1}/min.

The results in Figure 4, particularly the comparison between parts b and d, indicate that in aerobic samples of cytochrome oxidase, the photoreduction process leads first to reduction of cytochrome *a* followed by reduction of cytochrome a_3. This redox situation, i.e., reduced cytochrome *a* and oxidized cytochrome a_3, corresponds to that found in the aerobic steady state (Nicholls & Petersen, 1974) and suggests the following mechanism for the photoreduction process. Illumination produces reducing equivalents external to the oxidase [most likely via a flavin contamination (Adar & Yonetani, 1978)] which subsequently reduce the enzyme. In the presence of oxygen, the predominant species is that corresponding to the aerobic steady state ($a^{2+}a_3^{3+}$). Upon depletion of O_2, full reduction is achieved (Adar & Yonetani, 1978). This proposal is compatible with our previous results with 441.6-nm excitation which showed minimal formation of reduced cytochrome a_3 upon illumination of static oxidase samples (Salmeen et al., 1978), with the observations of Adar & Erecińska (1979), who saw a delay in the appearance of the 1665-cm^{-1} band, characteristic of reduced cytochrome a_3, in the initial stages of photoreduction at −10 °C, and with the results of Bocian et al. (1979) who showed that Soret excitation of frozen oxidase samples produced photoreduction but that visible excitation did not. This latter result is expected if the photoactive species is a flavin, which has strong absorption in the blue but not in the red region ($\lambda > 550$ nm) of the spectrum.

We have studied the photoreduction process in more detail by carrying out laser-power studies on flowing oxidase samples (Figure 5). At low to moderate powers of 406.7- and 413.1-nm excitation (Figure 5a,b,c) the spectrum of the oxidized enzyme is observed. Only at 55-mW incident power do photoreduction effects, notably the increase in intensity of

[3] G. T. Babcock, unpublished observations.

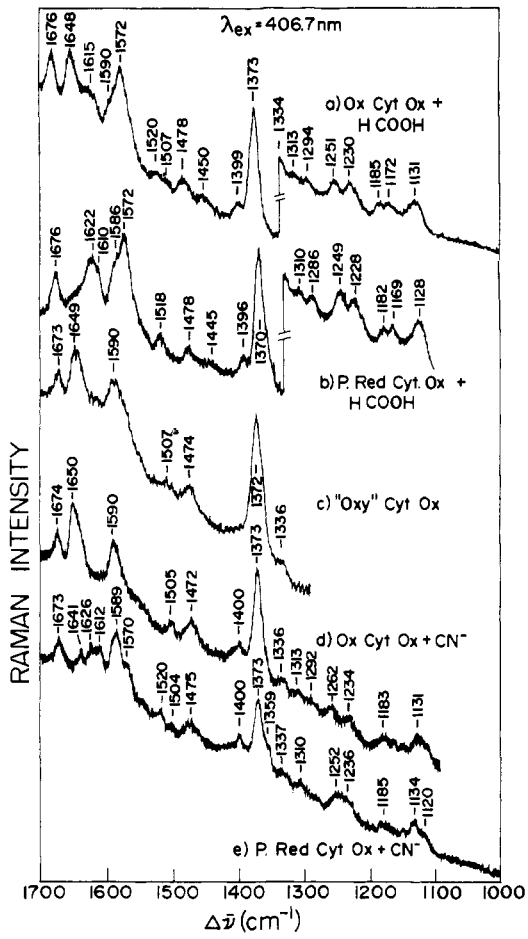

FIGURE 6: Resonance Raman spectra of oxidized (a and d) and partially reduced (b and e) complexes of cytochrome oxidase with formate and cyanide. In (c) the spectrum of oxygenated cytochrome oxidase, formed by air oxidation of the dithionite reduced enzyme, is shown. Instrumental conditions: resolution, 6 cm^{-1}; time constant, 1 s; scan rate, 50 cm^{-1}/min.

bands at 1622, 1610, and 1520 cm^{-1}, become evident. These spectra demonstrate that the use of the oxidation-state marker band as a judge of photoreduction is a poor criterion. Even with appreciable photoreduction (Figure 5d) there is little obvious change in this band. This observation, as well as the fact that photoreduction produces its first noticeable effects in the 1600-cm^{-1} region with 406.7- and 413.1-nm excitation, can be rationalized by reference to the excitation profile data presented above. Under conditions of partial photoreduction the predominant form of the enzyme is indentified as the aerobic steady state: cytochrome a_3 oxidized and cytochrome a reduced. The a^{2+} species has an absorption peak at 443 nm which is 2015 and 1634 cm^{-1} to the red of the 406.7- and 413.1-nm laser lines, respectively. Consequently, from eq 3 above, we expect that vibrations in these frequency regions will be more strongly enhanced than those to lower frequency and that photoreduction will be apparent first in the high-frequency modes. As more of the enzyme is reduced, this process also becomes evident in the 1360-cm^{-1} region (Figure 4c). These excitation profile arguments also rationalize our earlier observations on the photoreduction of the oxidized enzyme (Salmeen et al., 1978) in which excitation at 441.6 nm (72 cm^{-1} from the 443-nm a^{2+} peak absorption) resulted in the observation of cytochrome a^{2+} modes throughout the Raman spectrum.

Raman Spectra of Inhibitor Complexes of Cytochrome Oxidase and of Its Oxygenated Form. Figure 6 presents Raman spectra of several derivatives of cytochrome oxidase; the vibrational assignments we have deduced from these data are summarized in Table I. In the formate complex of the oxidized enzyme, cytochrome a_3^{3+}·HCOOH is high-spin whereas cytochrome a^{3+} remains low-spin (Babcock et al., 1976). There is thus no change in spin state in going from the resting enzyme to the formate complex, and correspondingly the Raman spectra of these two oxidase species are similar (compare Figure 4a with Figure 6a). Upon reduction of cytochrome a in the presence of formate, the mixed valence species $a^{2+}a_3^{3+}$·HCOOH is formed (Figure 6b). The a_3^{3+}·HCOOH bands at 1676, 1572, and 1478 cm^{-1} remain constant whereas the oxidized a bands at 1648, 1590, and 1507 cm^{-1} are replaced by bands at 1622, 1610, 1586, and 1518 cm^{-1} as reduction of cytochrome a occurs. Upon CN^- addition to the oxidized enzyme, the species $a^{3+}a_3^{3+}$·CN is formed and the a and a_3 species occur in the low-spin state. In the Raman spectrum of this derivative (Figure 6d), the high-spin a_3^{3+} band at 1572 cm^{-1} is absent and both a^{3+} and a_3^{3+}·CN^- show the low-spin ferric heme a marker band at 1590 cm^{-1}. The 1478-cm^{-1} high-spin band of the oxidized enzyme is also absent, having been replaced by the low-spin band at 1505 cm^{-1}. The latter change is somewhat obscured by the appearance of the 1472-cm^{-1} band which occurs in low-spin heme a^{3+} complexes (Callahan & Babcock, 1981). Upon reduction of cytochrome a in the oxidized, cyanide-complexed enzyme, the mixed valence species $a^{2+}a_3^{3+}$·CN is formed (Figure 6e). As with the partially reduced formate species, the a^{2+} modes at 1626, 1610, 1520, and 1359 cm^{-1} appear. The low-spin a_3^{3+}·CN^- modes remain at 1673, 1641, 1589, 1504, 1475, and 1373 cm^{-1}.

As we noted above some forms of the cytochrome oxidase species collectively referred to as "oxygenated" (Orii & King, 1976) are generated during irradiation of the oxidized enzyme in the flowing sample cell. These species are characterized by a Soret peak at 427 mm and have received renewed attention recently owing to the kinetic observations of Chance, Beinert, and their co-workers (Chance et al., 1978; Shaw et al., 1978). Figure 6c shows the Raman spectrum we observe for oxygenated cytochrome oxidase generated by dithionite reduction of the enzyme in cholate detergent and subsequent air oxidation. The 1572-cm^{-1} peak characteristic of cytochrome a_3^{3+} in the resting enzyme is absent in this species; the major band in the spin marker region occurs at 1590 cm^{-1}, typical of low-spin, six-coordinate heme a^{3+}. Overall, the spectrum of the oxygenated species generated by the classic technique we have used bears a strong resemblance to that of the oxidized enzyme in the presence of cyanide.

Discussion

Optical Properties of Oxidase and Excitation Profile. The Raman data presented here and elsewhere (Salmeen et al., 1978; Babcock & Salmeen, 1979; Ondrias & Babcock, 1980), as well as the Raman observations made by Woodruff et al., (1981), provide strong evidence in support of Vanneste's (Vanneste, 1966) original decomposition of the optical properties of cytochrome oxidase into separate cytochrome a and a_3 contributions (Table I). Thus laser excitation (441.6 nm) on the long-wavelength side of the oxidized oxidase Soret band generates the Raman spectrum of cytochrome a^{3+} (Babcock & Salmeen, 1979). Laser excitation (413.1 nm, 406.7 nm) on the short-wavelength side produces the Raman spectrum of cytochrome a_3^{3+} through the first term of eq 3 and those vibrational modes of cytochrome a^{3+} which are in resonance according to the second term of this equation. The cytochrome a^{3+} absorption peak occurs at 427 nm, which is 790 cm^{-1} away from the 413.1-nm krypton line. Consequently, the observation

Table I: Optical, Coordination, and Vibrational Properties of Cytochrome a and a_3 in Various Cytochrome Oxidase Species

species	spin	coordination	λ_{max}	characteristic vibrations (cm^{-1})
a_3^{3+}	5/2	6	414	1373, 1478, 1572, ~1615, 1676
a_3^{3+}·HCOOH	5/2	6	414	1373, 1478, 1572, ~1615, 1676
a_3^{3+}·CN	1/2	6	427	1373, 1474, 1506, 1590, 1641, 1676
a^{3+}	1/2	6	427	1373, 1474, 1506, 1590, 1641, 1650
a^{2+}	0	6	443	1358, 1521, 1622,
a_3^{2+}	2	5	443	215, 364, 1230, 1358, 1472, 1666
heme $a^{3+}Cl^-$ [a]	5/2	5	414	1374, 1492, 1581, 1632, 1676
heme $a^{3+}(Me_2SO)_2$ [a]	5/2	6	410	1373, 1482, 1572, 1615, 1672
heme $a^{3+}(NMeIm)_2$ [a]	1/2	6	422	1374, 1474, 1506, 1590, 1642, 1670

[a] From Callahan & Babcock (1981).

that the low-frequency modes in the Raman spectrum of the oxidized enzyme obtained with 413.1-nm excitation are those of cytochrome a_3^{3+} (Ondrias & Babcock, 1980; Woodruff et al., 1981) can be rationalized.

Coordination Geometries of a and a_3 in Various Cytochrome Oxidase Species. With the Raman data presented here and in the previous paper (Callahan & Babcock, 1981), we are able to assign geometries for the principal cytochrome oxidase species (Table I). Cytochrome a is low-spin in both valence states (Tweedle et al., 1978), and consequently six-coordination is expected. This expectation is borne out by a comparison between the Raman properties of $(NMeIm)_2$ heme a^{3+} and those of cytochrome a^{3+} in the 1500–1600-cm^{-1} region and is in agreement with earlier EPR (Blumberg & Peisach, 1979; Babcock et al., 1979) and MCD (Nozawa et al., 1979) observations. An interesting anomaly for cytochrome a involves the behavior of its formyl group. The formyl vibration is observed in the $(NMeIm)_2$ heme a^{3+} model compound at 1676 cm^{-1}. For cytochrome a^{3+}, however, the highest frequency mode is observed at 1650 cm^{-1} with a second vibration apparent at 1641 cm^{-1} (Figure 4a; Babcock & Salmeen, 1979).[4] Thus, even though the $(NMeIm)_2$heme a^{3+} species has the EPR crystal field parameters of cytochrome a^{3+}, it does not have the vibrational properties of the in vivo formyl group. We are in the process of exploring the basis for this unusual behavior.

Because cytochrome a_3^{3+} is high-spin (Tweedle et al., 1978) and can exist as either five- or six-coordinate, the model compound data for heme a are extremely useful in the determination of its geometry. In the resting enzyme cytochrome a_3^{3+} contributes vibrations at 1676, 1572, and 1478 cm^{-1} in the high-frequency region. A weak feature near 1615 cm^{-1} may also be due to the a_3^{3+} chromophore (Figure 4a). A comparison of these frequency positions with those of the high-spin five- and six-coordinate model compounds of Table

[4] That the highest frequency band attributed to cytochrome a^{3+} occurs at 1650 cm^{-1} suggests that a covalent interaction between the formyl group of this heme a chromophore and the protein may be involved. A protonated Schiff's base linkage could account for these observations (Ondrias & Babcock, 1980) and may play a role in the proton pump activity of cytochrome oxidase.

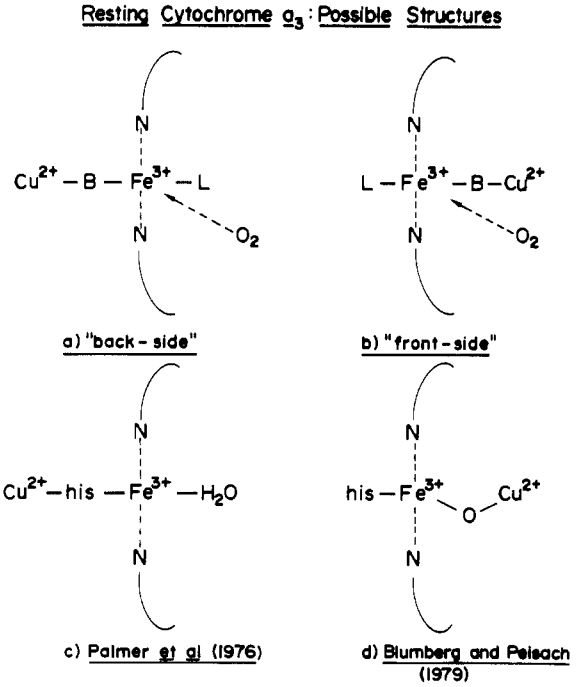

FIGURE 7: Possible structures for cytochrome a_3 dioxygen reducing site. See text for details.

I clearly shows that the heme $a^{3+}(Me_2SO)_2$ complex reproduces the cytochrome a_3^{3+} spectrum well; the five-coordinate model, heme $a^{3+}Cl^-$, does so much less adequately. Thus, we conclude that in the resting enzyme, the a_3^{3+} species occurs in the high-spin, six-coordinate state. Table I also indicates that the frequency positions assigned to the a_3^{3+}·CN^- complex and those of the low-spin heme $a^{3+}(NMeIm)_2$ compare well, confirming the assignment of cyanide derivative as six coordinate and low-spin. Finally a_3^{3+}·HCOOH can be seen to occur as the six-coordinate high-spin species consistent with the idea that formate serves as a ligand to the iron in this inhibitor complex (Nicholls, 1976).

Our finding that cytochrome a_3^{3+} in the resting enzyme is six coordinate has interesting ramifications with respect to the structure of the oxygen reducing site and the mode by which the proposed exchange coupling between the iron of a_3 and the associated copper (Van Gelder & Beinert, 1969; Palmer et al., 1976) is mediated. Two general models are available in the literature [as well as a proposal which eliminates the need for exchange coupling altogether; see Seiter & Angelos (1980)]. These can be classified as "back-side" bridging in which the copper is coupled to the iron via a ligand on the opposite side of the heme a ring to which O_2 binding occurs and "front-side" bridging in which the copper is coupled to the iron by a ligand which occupies the reduced protein dioxygen binding site (see Figure 7a,b). A specific back-side model has been proposed in which the bridging ligand is a histidine residue (Palmer et al., 1976). This is represented in Figure 7c where we have also incorporated a water molecule in the iron sixth ligand position to account for the Raman data we have presented. A front-side model has also been proposed which postulates a μ-oxo bridging ligand (Blumberg & Peisach, 1979) and is shown in Figure 7d; here we have incorporated a histidine residue as the sixth ligand to maintain the iron in the six-coordinate state. These models are somewhat speculative; for example, a water molecule or other ligand could substitute for the histidine in Figure 7d.

At present, convincing evidence is available for neither of these models, and each has weaknesses as well as strengths. For example, the histidine, back-side bridge has been criticized

since imidazole bridging ligands are generally unable to support exchange coupling with magnitudes as large as those found in the oxidase ($-2J > 200$ cm^{-1}) [Kolks et al., 1976; Landrum et al., 1978; Haddad & Hendrickson, 1978; Petty et al., 1980; see, however, Desideri et al. (1978)], whereas μ-oxo exchange couplings are well within this range (O'Keeffe et al., 1975). On the other hand, the occurrence of six-coordinate, high-spin iron with histidine and water in the fifth and sixth coordination sites in the back-side model has ample precedent from aquometmyoglobin and aquomethemoglobin. Heme in-plane iron with a μ-oxo ligand, however, is a unique structure in the front-side model since a μ-oxo ligand generally forces the iron to adopt a five-coordinate, out of plane geometry (O'Keeffe et al., 1975). In this regard, Seiter has suggested other ligands, in particular carbonate, in place of the μ-oxo bridge in a front-side model (Seiter, 1978). Perhaps the most obvious method to distinguish between the possibilities suggested by Figure 7 is the determination of the magnetic susceptibility of the oxidized enzyme–formate complex. Formation of this complex would be only a slight perturbation to the structure of part c of Figure 7 whereas for part d one might expect this ligand to displace the μ-oxo species and drastically alter the exchange coupling.

In the transition from oxidized to oxygenated oxidase, the polarized core size indicator band for cytochrome a_3^{3+} shifts from 1572 cm^{-1} to a frequency close to 1590 cm^{-1} (Figure 6c) and indicates that the C_t–N distance decreased during the process (Callahan & Babcock, 1981). It is somewhat difficult to quantify this frequency decrease since the observed spectrum also contains contributions from a^{3+} which obscure the exact location of the a_3^{3+} band. A transition to the five-coordinate, high-spin state can be ruled out, however, since this species is also expected to show a vibrational mode in the band II region at 1492 cm^{-1} (see Figure 5a in the preceding paper). The only bands in this region occur at 1507 and 1474 cm^{-1}, characteristic of the six-coordinate, low-spin state, and we conclude that the geometry of cytochrome a_3^{3+} in the oxygenated enzyme closely resembles that of a low-spin ferric heme a species. However, the MCD spectrum of oxygenated oxidase is essentially identical with that of the oxidized enzyme (Babcock et al., 1976), whereas the transition from high-spin a_3^{3+} in the resting enzyme to a low-spin species in the oxygenated form is expected to produce a large intensity increase in the Soret MCD (Vickery et al., 1976). The resolution of this paradox may lie in the EPR properties of the oxygenated form elucidated recently by Shaw et al. (1978). The observed spectrum is unusual in that the principal g values occur at $g = 5.0$, 1.78, and 1.69 and is thought to arise from a spin-coupled system. Therefore it is possible that in this species cytochrome a_3^{3+} has assumed a low-spin geometry with a contracted porphyrin core but remains magnetically coupled to the $Cu_{a_3}^{2+}$. The magnetic coupling may produce a perturbation to the π^* states sufficient to quench the MCD (Treu & Hopfield, 1975).

In the reduced protein, only cytochrome a_3^{2+} is paramagnetic and occurs in the high-spin state. The MCD properties of this species are quite similar to those of deoxyhemoglobin and deoxymyoglobin (Babcock et al. 1976) as are its ligand binding properties (Erecińska & Wilson, 1978). These observations suggest that a_3^{2+} is five-coordinate in the reduced enzyme in the absence of an added ligand. This conclusion is consistent with our previous Raman results which identified specific vibrations associated with a_3^{2+} (Salmeen et al., 1978) including a vibration at 215 cm^{-1}. This mode behaves in a manner similar to the 215-cm^{-1} vibration in deoxyhemoglobin and deoxymyoglobin which has been assigned to the iron–histidine nitrogen stretching mode (Nagai et al., 1980; Hori & Kitagawa, 1980).

An additional conclusion can be reached concerning the nature of the a_3 site from the Raman results presented here and in previous reports (Salmeen et al., 1978; Ondrias & Babcock, 1980; Babcock & Salmeen, 1979). In both the oxidized and reduced states of the enzyme the formyl vibration of a_3 is clearly enhanced and occurs at a frequency typical of a free, non-hydrogen-bonded C=O. These observations indicate that the a_3 site, at least in the vicinity of pyrrole ring IV, is hydrophobic and that bulk H_2O is excluded.

One of the observations used by Seiter & Angelos (1980) in support of their postulate of Fe(IV) at the cytochrome a_3 site in the resting enzyme is the susceptibility of the enzyme to photoreduction. They suggested that the a_3 site, due to its postulated ferryl nature, was directly photoreducible. The results on photoreduction reported here argue against this interpretation since they show that the cytochrome a site is the locus of photoreduction effects. The results of Bocian et al. (1979) which demonstrate the lack of photoreduction with α-band excitation also argue against direct photochemistry at the cytochrome a_3 site. They instead are consistent with the flavin photoreduction mechanism originally proposed by Adar & Yonetani (1978) and favored by us in the interpretation of our data. In general we have found no evidence to suggest that a_3 in the resting enzyme is in any valence state but the ferric; we can mimic the Raman properties of the enzyme iron centers of the oxidized enzyme well with relatively simple ferric heme a model compounds. We have not yet, however, prepared ferryl heme a model compounds to test directly the proposed occurrence of this species in the enzyme. Conclusive evidence should come from studies of this nature.

Acknowledgments

We thank Drs. S. I. Chan, J. A. Shelnutt, and W. H. Woodruff for communicating results in advance of publication and Professor Woodruff for helpful discussions on the coordination geometry of cytochrome a_3.

References

Adar, F., & Yonetani, T. (1978) *Biochim. Biophys. Acta 502*, 80–86.

Adar, F., & Erecińska, M. (1979) *Biochemistry 18*, 1825–1829.

Albrecht, A. C., & Hutley, M. C. (1971) *J. Chem. Phys. 55*, 4438–4443.

Babcock, G. T., & Salmeen, I. (1979) *Biochemistry 18*, 2493–2498.

Babcock, G. T., Vickery, L. E., & Palmer, G. (1976) *J. Biol. Chem. 251*, 7907–7919.

Babcock, G. T., Vickery, L. E., & Palmer, G. (1978) *J. Biol. Chem. 253*, 2400–2411.

Babcock, G. T., Van Steelandt, J., Palmer, G., Vickery, L. E., & Salmeen, I. (1979) *Dev. Biochem. 5*, 105–115.

Babcock, G. T., Callahan, P. M., McMahon, J. J., Ondrias, M. R., & Salmeen, I. (1980) *Proc. Symp. Interact. Iron Proteins Oxygen Electron Transp.* (in press).

Blumberg, W. E., & Peisach, J. (1979) *Dev. Biochem. 5*, 153–159.

Bocian, D. F., Lemley, A. T., Petersen, N. O., Brudvig, G. W., & Chan, S. I. (1979) *Biochemistry 18*, 4396–4402.

Brudvig, G. W., Stevens, T. H., & Chan, S. I. (1980) *Biochemistry 19*, 5275–5285.

Callahan, P. M., & Babcock, G. T. (1981) *Biochemistry 20* (preceding paper in this issue).

Champion, P. M., & Albrecht, A. C. (1979) *J. Chem. Phys. 71*, 1110–1121.
Chance, B., Saronio, C., Leigh, J. S., Jr., Ingledew, W. J., & King, T. E. (1978) *Biochem. J. 171*, 787–798.
Clark, R. J. H., & Stewart, B. (1979) *Struct. Bonding (Berlin) 36*, 1–80.
Desideri, A., Cerdonio, F., Mogno, F., Vitale, S., Calabrese, L., Cocco, D., & Rotillo, G. (1978) *FEBS Lett. 89*, 83–85.
Erecińska, M., & Wilson, D. F. (1978) *Arch. Biochem. Biophys. 188*, 1–14.
Felton, R. H., & Yu, N.-T. (1978) *Porphyrins 3*, 347–393.
Friedman, J. M., Rousseau, D. L., & Adar, F. (1977) *Proc. Natl. Acad. Sci. U.S.A. 74*, 2607–2611.
Haddad, M. S., & Hendrickson, D. N. (1978) *Inorg. Chem. 17*, 2622–2630.
Hori, H., & Kitagawa, T. (1980) *J. Am. Chem. Soc. 102*, 3608–3613.
Kolks, G., Frihart, C. R., Rabinowitz, H. N., & Lippard, S. J. (1976) *J. Am. Chem. Soc. 98*, 5720–5721.
Landrum, J. T., Reed, C. A., Hatano, K., & Scheidt, W. R. (1978) *J. Am. Chem. Soc. 100*, 3232–3233.
Malmström, B. G. (1979) *Biochim. Biophys. Acta 549*, 281–303.
Nafie, L. A., Pezolet, M., & Peticolas, W. L. (1973) *Chem. Phys. Lett. 20*, 563–568.
Nagai, K., Kitagawa, T., & Morimoto, H. (1980) *J. Mol. Biol. 136*, 271–289.
Nicholls, P. (1976) *Biochim. Biophys. Acta 430*, 13–29.
Nicholls, P., & Petersen, L. C. (1974) *Biochim. Biophys. Acta 357*, 462–467.
Nozawa, T., Orii, Y., Kaito, A., Yamamoto, T., & Hatano, M. (1979) *Dev. Biochem. 5*, 117–128.
O'Keeffe, D. H., Barlow, C. H., Symthe, G. A., Fuchsman, W. H., Moss, T. H., Lilienthal, H. R., & Caughey, W. S. (1975) *Bioinorg. Chem. 5*, 125–147.
Ondrias, M. R., & Babcock, G. T. (1980) *Biochem. Biophys. Res. Commun. 93*, 29–35.
Orii, Y., & King, T. E. (1976) *J. Biol. Chem. 251*, 7487–7493.
Palmer, G., Babcock, G. T., & Vickery, L. E. (1976) *Proc. Natl. Acad. Sci. U.S.A. 73*, 2206–2210.
Petty, R. H., Welch, B. R., Wilson, L. J., Bottomley, L. A., & Kadish, K. M. (1980) *J. Am. Chem. Soc. 102*, 611–620.
Reed, C. A., & Landrum, J. T. (1979) *FEBS Lett. 106*, 265–267.
Rousseau, D. L., Friedman, J. M., & Williams, P. F. (1979) *Top. Curr. Phys. 11*, 203–252.
Salmeen, I., Rimai, L., Gill, D., Yamamoto, T., Palmer, G., Hartzell, C. R., & Beinert, T. H. (1973) *Biochem. Biophys. Res. Commun. 52*, 1100–1107.
Salmeen, I., Rimai, L., & Babcock, G. T. (1978) *Biochemistry 17*, 800–806.
Seiter, C. H. A. (1978) *Front. Biol. Energ.* [*Pap. Int. Symp.*], 798–804.
Seiter, C. H. A., & Angelos, S. G. (1980) *Proc. Natl. Acad. Sci. U.S.A. 77*, 1806–1808.
Shaw, R. W., Hansen, R. E., & Beinert, H. (1978) *J. Biol. Chem. 253*, 6637–6640.
Shelnutt, J. A. (1980) *J. Chem. Phys. 72*, 3948–3958.
Shelnutt, J. A., O'Shea, D. C., Yu, N.-T., Cheung, L. D., & Felton, R. H. (1976) *J. Chem. Phys. 64*, 1156–1165.
Spaulding, L. D., Chang, C. C., Yu, N.-T., & Felton, R. H. (1975) *J. Am. Chem. Soc. 97*, 2517–2525.
Spiro, T. G., Stong, J. D., & Stein, P. (1979) *J. Am. Chem. Soc. 101*, 2648–2655.
Stevens, T. H., Brudvig, G. W., Bocian, D. F., & Chan, S. I. (1979) *Proc. Natl. Acad. Sci. U.S.A. 76*, 3320–3324.
Treu, J. I., & Hopfield, J. J. (1975) *J. Chem. Phys. 63*, 613–623.
Tweedle, M. F., Wilson, L. J., García-Iñiguez, L., Babcock, G. T., & Palmer, G. (1978) *J. Biol. Chem. 253*, 8065–8071.
Van Gelder, B. F., & Beinert, H. (1969) *Biochim. Biophys. Acta 189*, 1–24.
Vanneste, W. H. (1966) *Biochemistry 5*, 838–848.
Vickery, L., Nozawa, T., & Sauer, K. (1976) *J. Am. Chem. Soc. 98*, 343–350.
Wikström, M., & Krab, K. (1979) *Biochim. Biophys. Acta 549*, 177–222.
Woodruff, W. H., Dallinger, R. F., Antalis, T. M., & Palmer, G. (1981) *Biochemistry* (in press).